



저작자표시-비영리-변경금지 2.0 대한민국

이용자는 아래의 조건을 따르는 경우에 한하여 자유롭게

- 이 저작물을 복제, 배포, 전송, 전시, 공연 및 방송할 수 있습니다.

다음과 같은 조건을 따라야 합니다:



저작자표시. 귀하는 원저작자를 표시하여야 합니다.



비영리. 귀하는 이 저작물을 영리 목적으로 이용할 수 없습니다.



변경금지. 귀하는 이 저작물을 개작, 변형 또는 가공할 수 없습니다.

- 귀하는, 이 저작물의 재이용이나 배포의 경우, 이 저작물에 적용된 이용허락조건을 명확하게 나타내어야 합니다.
- 저작권자로부터 별도의 허가를 받으면 이러한 조건들은 적용되지 않습니다.

저작권법에 따른 이용자의 권리는 위의 내용에 의하여 영향을 받지 않습니다.

이것은 [이용허락규약\(Legal Code\)](#)을 이해하기 쉽게 요약한 것입니다.

[Disclaimer](#)

Evaluation of Electrical Stimulator to Enhance Spinal Fusion in a Rat Posterolateral Spinal Fusion Model

Gyu Yeul Ji

Department of Medicine
The Graduate School, Yonsei University

Evaluation of Electrical Stimulator to Enhance Spinal Fusion in a Rat Posterolateral Spinal Fusion Model

Directed by Professor Keung Nyun Kim

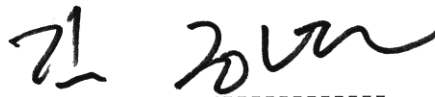
The Doctoral Dissertation
submitted to the Department of Medicine
the Graduate School of Yonsei University
in partial fulfillment of the requirements for the degree of
Doctor of Philosophy

Gyu Yeul Ji

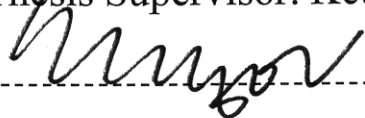
December 2017



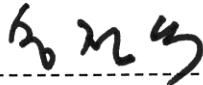
This certifies that the Doctoral Dissertation
of Gyu Yeul Ji is approved



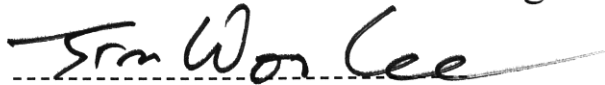
Thesis Supervisor: Keung Nyun Kim



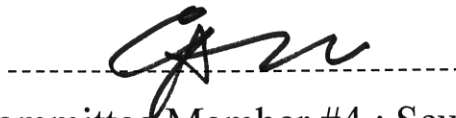
Thesis committee Member #1 : Dong Ah Shin



Thesis committee Member #2 : Jung Sik Song



Thesis committee Member #3 : Jin Woo Lee



Thesis committee Member #4 : Seung Hwan Yoon

The Graduate School
Yonsei University

December 2017

ACKNOWLEDGEMENTS

This dissertation would not have been possible without the guidance and the help of several individuals who in one way or another contributed and extended their valuable assistance in the completion of this study. In the first place, I would like to record my gratitude to my supervisor, Professor Keung Nyun Kim for his supervision, advice, and guidance from the very early stage of this research as well as giving me extraordinary experiences throughout the work. I also convey special acknowledgement to Professor Do Heum Yoon, Professor Yoon Ha, Professor Seong Yi, and Professor Dong Ah Shin for providing me encouragement and helpful advice in numerous ways. Especially, I would like to thanks to my parents. Without their endless devotion and love, I would not have finished the degree. Finally, not the least, I would like to express my sincere thanks to my wife who constantly inspire me and support me in various ways. In addition, I love my daughter, Rachael, who always makes me happy. It was a great accomplishment of mine that I broaden my academic knowledge and upgrading my experimental skill while completing the thesis. Based on it, I hope it will contribute to the advance of the fusion based spinal surgery.

Gyu Yeul Ji

<TABLE OF CONTENTS>

ABSTRACT	1
I. INTRODUCTION	3
II. MATERIALS AND METHODS	
1. Fabrication of nitinol mesh and electrical stimulator	5
2. Culture of human mesenchymal stem cell-like cells on nitinol mesh.....	7
3. Characterization of human mesenchymal stem cell-like cells	8
4. Animal model and surgical procedure	9
5. Microcomputerized tomographic scan	14
6. Gross palpation and manual testing	14
7. Biomechanical testing	15
8. Histological examination	16
9. Molecular analysis	17
10. Statistical analysis	17
III. RESULTS	
1. Characterization of human mesenchymal stem cell-like cells	18
2. Microcomputerized tomographic scan	21
3. Manual assessment of fusion	22
4. Biomechanical testing.....	23
5. Histological examination	24
6. Molecular analysis	26
IV. DISCUSSION	27
V. CONCLUSION	30
REFERENCES.....	31
ABSTRACT (IN KOREAN)	35

LIST OF FIGURES

Figure 1A. Nitinol mesh container and two electrical stimulators	6
Figure 1B. Circuit diagram of the electrical stimulator	6
Figure 2. Design of Chamber, nitinol mesh and DC stimulation set up	8
Figure 3A. Morselized iliac bone graft was placed inside nitinol mesh, and nitinol meshes were connected to electrical stimulator.....	11
Figure 3B. Two nitinol containers were implanted on posterior decorticated transverse process surfaces on both sides using one type of DC stimulator	11
Figure 3C. Lumbar spine was extracted 8 weeks after surgery for fusion assessment	12
Figure 4. Schematic illustration of rat posterolateral fusion	13
Figure 5. Biomechanical assessment of fusion mass at 8 weeks after posterolateral spinal fusion (PLF) using three-point bending test	15
Figure 6. Microscopic images of the target cells	
Figure 6A. Microscopic images of hMSC-LC cultured on nitinol mesh	19
Figure 6B. Immunostaining of cultured groups	19
Figure 6C. Alkaline phosphate staining	20
Figure 6D. Alizarin red staining	20

Figure 7. Microcomputed tomography analysis on volume of newly formed bone at 8 weeks after posterolateral fusion	22
Figure 8. Biomechanical assessment of fusion mass at 8 weeks after posterolateral fusion (PLF) using three-point bending test	23
Figure 9. Histological staining of fusion mass at 8 weeks after posterolateral fusion	25
Figure 10. Protein analysis of obtained tissues	26

LIST OF TABLES

Table 1. Features of electrical stimulators	7
Table 2. Group description	14

ABSTRACT

Evaluation of electrical stimulator to enhance spinal fusion in a rat posterolateral spinal fusion model

Gyu Yeul Ji

*Department of Medicine
The Graduate School, Yonsei University*

(Directed by Professor Keung Nyun Kim)

BACKGROUND CONTEXT: Posterolateral fusion (PLF) with autogenous iliac bone graft is one of the most commonly performed surgical procedures for lumbar spinal disease. However, its limited success demands new biologically competent graft enhancers or substitutes. Although the use of direct current (DC) electrical stimulation has been shown to increase rate of successful spinal fusions, little is known about the effects of using different types of currents in DC stimulation.

PURPOSE: This study evaluated the effects of various DC stimulators on strength and success rate of posterolateral fusion in rats, using nitinol mesh container.

STUDY DESIGN: This was an experimental animal study.

METHODS: Electrified tubular nitinol mesh container was used to carry small pieces of bone grafts. Nitinol mesh container received electrical stimulation via lead that connected bone container to different types of DC stimulators. Sixty Sprague-Dawley male rats underwent posterolateral fusion between L4 and L5 transverse processes with bilateral iliac grafts. A stimulator was implanted subcutaneously, and rats were divided into three groups: the nitinol container-only control group (N=20) that underwent PLF with nitinol container filled with autografts, the constant DC (100 μ A)

stimulator group with nitinol container (N=20), and the pulsed DC (100 μ A, 100 Hz, 200 μ s) stimulator group with nitinol container (N=20). Rats were sacrificed at 8 weeks after surgery, and lumbar spines were removed. Spinal fusion was evaluated by microcomputerized tomographic (Micro-CT) scan, manual testing, biomechanical testing, histological examination, and molecular analysis.

RESULTS: All cases in varied DC stimulator group achieved solid fusion, whereas 70% of nitinol container-only control group showed solid fusion. Radiographic images, biomechanical testing, histological examination, and molecular analysis showed increasing fusion from nitinol container-only control group to the constant, and then to pulsed DC stimulator group. Volume of new bone mass was significantly higher in pulsed DC (100 μ A, 100 Hz, 200 μ s) stimulator group ($p < 0.05$). Fusion mass was more solidly fused in pulsed DC stimulator group than in nitinol container-only control group ($p < 0.05$). Pulsed DC stimulator group had the least inflammatory response.

CONCLUSIONS: Pulsed DC electrical stimulation is efficacious in improving both strength and fusion rate in a rat spinal fusion model. In addition, it appears that a tubular nitinol mesh, made of electrified suture, is useful for holding small pieces of bone grafts and maintaining a good environment for bone fusion.

Key words: posterolateral fusion, nitinol mesh, electrical stimulation, constant direct current stimulation, pulsed direct current stimulation, human mesenchymal stem cell-like cells, osteogenic differentiation

Evaluation of electrical stimulator to enhance spinal fusion in a rat posterolateral spinal fusion model

Gyu Yeul Ji

*Department of Medicine
The Graduate School, Yonsei University*

(Directed by Professor Keung Nyun Kim)

I. Introduction

Posterolateral fusion (PLF) based surgery is the most common procedure for treating various spinal diseases.¹⁻⁴ The aim of PLF is to eliminate pain source arising from instability of motion segment, or to prevent progression of deformity in patients with instability, deformity, or degenerative lumbar spine disease. For this purpose, autogenous bone grafting has been considered the golden standard that shows osteoinductive, osteoconductive, and osteogenic properties.⁵ However, there are several procedure-related complications following autograft, such as donor site pain, infection, and hematoma.⁶ In addition, autograft cannot be used under certain conditions, such as poor bone quality of elderly patients, osteoporosis, malignancy, and previously extracted donor site.⁷ Although application of pedicle screw fixation has increased fusion rates, pseudoarthrosis has occurrence rate of nearly 40%, and it has been reported to cause persistent or recurrent pain and disability.⁸⁻¹⁰ Therefore, for several decades, researchers have explored ways to enhance fusion environment by mechanical or biological means.¹¹⁻¹⁵ However, such methods come with additional risks, and they have not completely eliminated pseudoarthrosis as a problem.¹⁶ An alternative method to enhance fusion environment is direct current (DC) electrical stimulation. Electrical stimulation, which has been widely studied regarding its effect

on bone healing, has an established role in the treatment of long-bone nonunions.¹⁷ Clinical efficacy of electrical stimulation for spinal fusion was first reported by Dwyer et al.¹⁸ in 1974. Several clinical studies showed that DC electrical stimulation enhances fusion success rates, particularly in “difficult to fuse” populations.^{19,20} Meril reported the use of adjunctive DC stimulation of allograft bone in lumbar interbody fusions.²¹ DC- stimulated group had an overall success rate of 93%, compared to 75% in non-stimulated group. Although DC electrical stimulation of spinal fusion has proven to be effective for increasing fusion rates in “high risk” patients, little information exists on the effect of DC stimulator in current type. The maintenance of a good healing environment for the maturation of bone fusion is important to increase the rate of spinal fusion. Prevention of soft-tissue interposition, easy migration of osteogenic cells, vascularization to the core of fusion mass, and mechanical stress are all important physiological factors that facilitate bone fusion.²² Previous studies, which used protective graft container made of polylactide sheath, demonstrated that fusion mass volume could be enhanced in a rabbit spinal fusion model.²³ Due to the undulating space between transverse processes, flexible container is preferred to fix it closely to the transverse processes in PLF. For better bone fusion, we assembled two different types of DC stimulators and a flexible bone container made of electrified tubular mesh that met the above mentioned physiological factors. The purpose of this study was to evaluate the effect of varied DC stimulator with nitinol container on bone fusion in a rat PLF model. We also investigated the biocompatibility of nitinol mesh container and varied DC stimulator during osteogenesis.

II. MATERIALS & METHODS

1. Fabrication of nitinol mesh and electrical stimulator

Nitinol mesh (S&G Biotech, Seoul, Korea) (Figure 1A) was used to transmit electrical stimulation and collect bone chips, and it was made of flexible nickel-titanium alloy stent which is typically used in heart surgery. Regular quadrilateral dimensions of 15 mm² were used *in vitro*, whereas cylindrical tube, which was 15 mm in length and 6 mm in diameter, with a mesh size of 2 mm were used *in vivo*. The nitinol meshes container was large in size, in order to allow cells to pass freely within it for better growth of blood vessels, and to prevent interposition of soft tissue between bone grafts. Sources of electric current were LM334 (Texas Instruments, Dallas, TX) and lithium battery (CR2032 and CR2430, Energizer, St. Louis, MO), which were used as power supplies (Figure 1A). Stimulators were designed by Cybermedic (Cybermedic, Iksan, Korea) (Figure 1B). Two types of stimulators using DC electronic circuits provided a constant (100 μ A) or pulsed (100 μ A, 100 Hz, 200 μ s) level DC to the nitinol mesh. Both constant and pulsed DC stimulators produced a mean voltage of 3V. The stimulators were coated with medical grade silicone (NuSil, Carpinteria, CA), which can prevent the internal environment of *in vivo* samples from getting exposed to electrical output and chemical byproduct created by the stimulator. Features of each stimulator are described in Table 1.

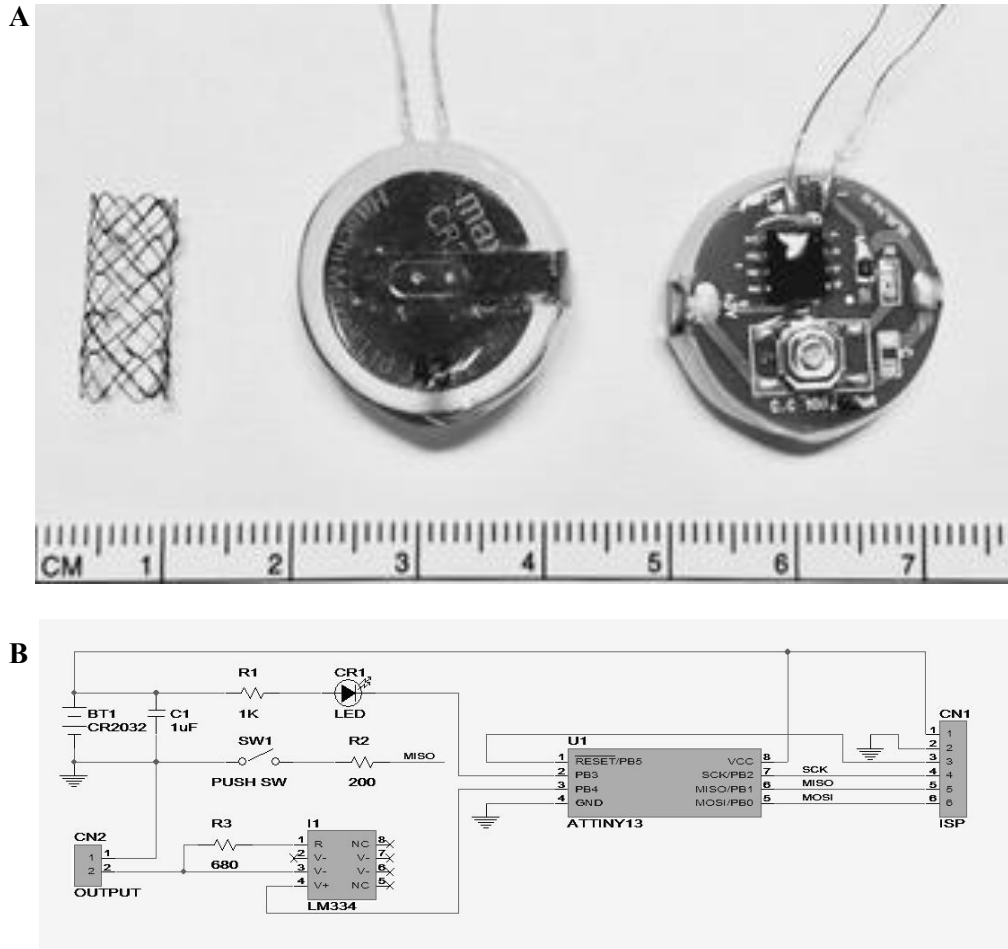
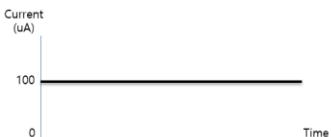
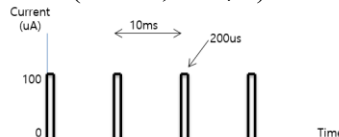


Figure 1. A. Nitinol mesh and two electrical stimulators (left: bottom, right: top).

B. Circuit diagram of electrical stimulator. Power button exists and status can be checked by LED lamp. C (capacitor) R (resister), V (voltage), SW (switch), PB (push button), GND (ground), VCC (supply voltage), SCK (serial clock), CR2032 (lithium battery), CR1 (LED lamp), LM334 (terminal adjustable current sources), ATTINY13 (AVR microcontroller), SCK (serial clock), MISO (master input, slave output), MOSI (master output, slave input)

Table 1. Features of electrical stimulators

Item	Constant DC	Pulsed DC
Output current	100 μA	100 μA
Output waveform	<p>Constant DC</p> 	<p>Pulsed DC (100 Hz, 200 μs)</p> 
Load resistance (constant current)	0~20 $\text{k}\Omega$	0~20 $\text{k}\Omega$
Input voltage	Lithium battery 3V (CR2032)	Lithium battery 3V (CR2430)
Power consumption	0.36 mW (Output)	0.54 mW (Output), 0.45 mW (Sleep)
Effective time	10 weeks	10 weeks
Size	20×20×6 mm	25×25×6 mm
Molding	MED-6640 (NuSil, Carpinteria, CA)	
Working condition	Works at 48 hours after switch went on	

2. Culture of human mesenchymal stem cell-like cells on nitinol mesh

To confirm the osteogenic effect of varied DC stimulation, *in vitro* experiment was designed. Human mesenchymal stem cell-like cells (hMSC-LCs) were obtained from adipose tissue. hMSC-LCs were cultured in a 75-cm² flask with MesenPro-RS™ basal medium (Thermo Fisher Scientific, Waltham, MA), 2% growth supplement, and 2-mM L-glutamine (Thermo Fisher Scientific, Waltham, MA) at 37°C in humid atmosphere with 5% CO₂. Medium changed every three days, and subcultures were typically performed every 14 days. Nitinol mesh was connected to cathodes and anodes of the varied DC stimulator. This device was fixed to Gosselin Petri Dish

design (Gosselin, Corning, NY) with four open compartments, which enables electron flow (Figure 2). All experiments ran for 4 weeks. Electrical stimulator delivered either constant (100 μ A) or pulsed (100 μ A, 100 Hz, 200 μ s) level of DC to nitinol mesh for 4 weeks. Constant and pulsed DC stimulators produced a mean voltage of 3V through nitinol mesh. hMSC-LCs were seeded on nitinol mesh at a density of 5×10^4 cells. One day after cell seeding, medium was changed to osteogenic differentiation. This medium contained StemPro[®] osteocyte differentiation basal medium (Invitrogen, Waltham, MA) and 5 μ g/ml gentamicin. Medium was changed two times per week.

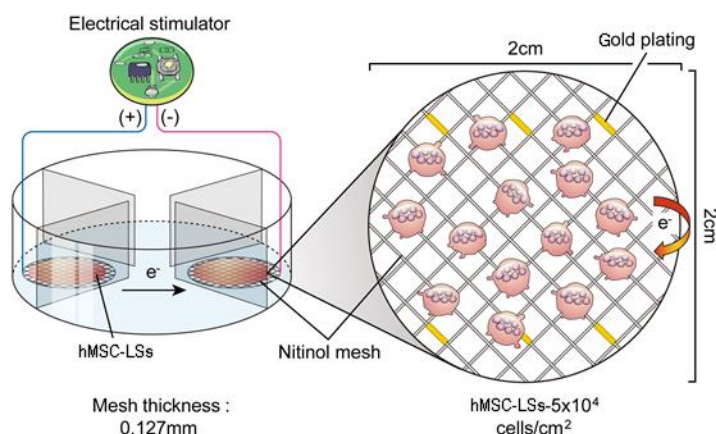


Figure 2. Design of chamber, nitinol mesh and DC stimulation set up. Illustration of osteogenic differentiation by DC stimulation *in vitro* using human mesenchymal stem cell-like cells.

3. Characterization of human mesenchymal stem cell-like cells

Immunocytochemistry: For immunostaining, hMSC-LCs were washed three times with Dulbecco's phosphate buffered saline (DPBS; Gibco, Grand Island, NY) for 5 minutes, and fixed with 4% paraformaldehyde (PFA) for 30 minutes. After fixation, cells were washed three times with phosphate buffered saline (PBS), and incubated with DPBS containing 0.3% Triton X-100 (Sigma-Aldrich, St. Louis, MO) for 10 minutes. Permeabilized cells were washed three times with DPBS for 5 minutes, incubated in DPBS containing 10% normal donkey serum (Jackson Laboratory, Barbor, ME) for 1

hour, and incubated overnight in anti-CD90 (1:250, Abcam, London, UK), anti-CD44 (1:100, Abcam), anti-RUNX2 (10 ug/ml, Abcam), anti-osteocalcin (1:80, Abcam), anti-Fibromodulin (5 ug/ml, Abcam), and anti-Sclerostin (5 ug/ml, Abcam) at 4°C. After washing, cells were incubated with secondary antibody conjugated with FITC or Cy3 for 1 hour. DAPI (4',6-diamidino-2-phenylindole)-conjugated mounting medium (Vector Laboratories, Burlingame, CA) was used for nuclei staining.

Alkaline phosphate staining: Cells were washed with DPBS for 5 minutes, and fixed with fixative solution (2% citrate: acetone=2:3) for 30 seconds. After fixation, cells were washed with distilled water for 1 minute. Then, cells were stained with alkaline-dye mixture (Fast blue RR salt, Naphthol AS-Mx phosphate alkaline solution, Sigma-Aldrich) for 1 hour, and washed three times with distilled water for 2 minutes. After washing, cells were stained Mayer's hematoxylin (Sigma-Aldrich) solution for 10 minutes, and washed with distilled water for 3 minutes. Cells were dried for two days after removing moisture.

Alizarin red staining: Following medium suction, hMSC-LCs were washed with DPBS for 5 minutes, and fixed with 10% formalin for 20 minutes. Cells were then washed three times with DPBS for 3 minutes. After washing, cells were stained with 2% alizarin red solution (Sigma-Aldrich) for 5 to 30 minutes, and washed three times with distilled water for 3 minutes. Cells were dried for two days after removing moisture.

4. Animal model and surgical procedure

In this study, we used 60 adult male Sprague Dawley rats (300 ± 15 g, mean ± standard deviation; OrientBio, Gyeonggi-do, Korea), housed in an animal facility permitted by Association for Assessment and Accreditation of Laboratory Animal Care (AAALAC). Rats were anesthetized with intraperitoneal ketamine (100 mg/kg; Yuhan, Seoul, Korea) and Rompun (10 mg/kg; Bayer, Leverkusen, Germany). Then, the animals were placed prone to Isotroy 100 (Troikaa Pharmaceuticals Limited, Gujarat, India) and shaved, while the operation side was sterilized with 10%

povidone-iodine solution. A dorsal midline incision was made, followed by two paramedian fascial incisions. An intermuscular plane between the multifidus and longissimus muscles was developed to expose transverse processes of L4 and L5, as well as intertransverse membrane. A low-speed drill was used to decorticate transverse processes and expose cancellous bone. To harvest graft bones, a lateral oblique incision was made along iliac crest on both sides. Then, all available corticocancellous bones were morselized with rongeurs, and weighed to create homogenous distribution of grafts between groups. Approximate weight of autologous iliac bone used in control group was 300 mg. Autogenous bone graft was placed within nitinol mesh (Figure 3A). The nitinol mesh container were placed between decorticated transverse processes in paraspinal bed (Figure 3B). Stimulator was placed subcutaneously. In the electrically stimulated group of animals, nitinol mesh received electrical stimulation by means of a lead connecting nitinol container to varied DC generator. Two types of current density, constant (100 μ A) and pulsed (100 μ A, 100 Hz, 200 μ s), were evaluated. DC current was applied to nitinol container for 8 weeks. Wounds were closed with 3-0 nylon sutures. Rats recovered from anesthesia in warm basket for 15 minutes, and were returned to home cages. Then, animals were observed twice daily throughout the post-surgical study period for general attitude, appetite, appearance of surgical site, neurological signs, and respiratory stress. Eight weeks after surgery, rats were euthanized by ketamine overdose. After euthanasia, lumbar spines were explanted from 1st lumbar vertebrae to sacral vertebrae, with surrounding musculatures intact (Figure 3C). Experimental design is outlined (Figure 4). Spinal fusion was assessed by Micro-CT scan evaluation, manual testing, biomechanical testing, as well as histological examination and molecular analyses. Rats were divided into three groups by implanting the following materials between transverse process of vertebra: (1) fusion with nitinol container-only as control group; (2) fusion with constant DC (100 μ A) stimulator with nitinol container as constant DC stimulator group; and (3) fusion with pulsed DC (100 μ A, 100 Hz, 200 μ s) stimulator with nitinol container as pulsed DC stimulator group.

Detailed data of each group are described in Table 2.

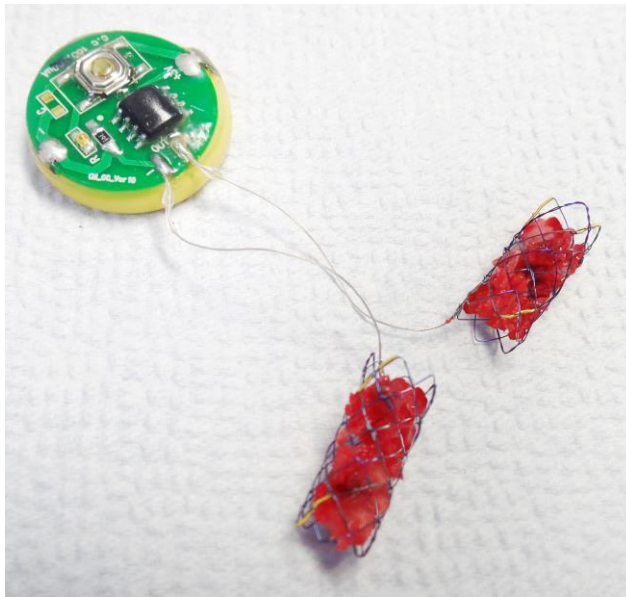


Figure 3A. Morselized iliac bone graft was placed inside nitinol mesh, and nitinol meshes were connected to electrical stimulator.



Figure 3B. Two nitinol containers were implanted on posterior decorticated transverse process surfaces on both sides using one type of DC stimulator.

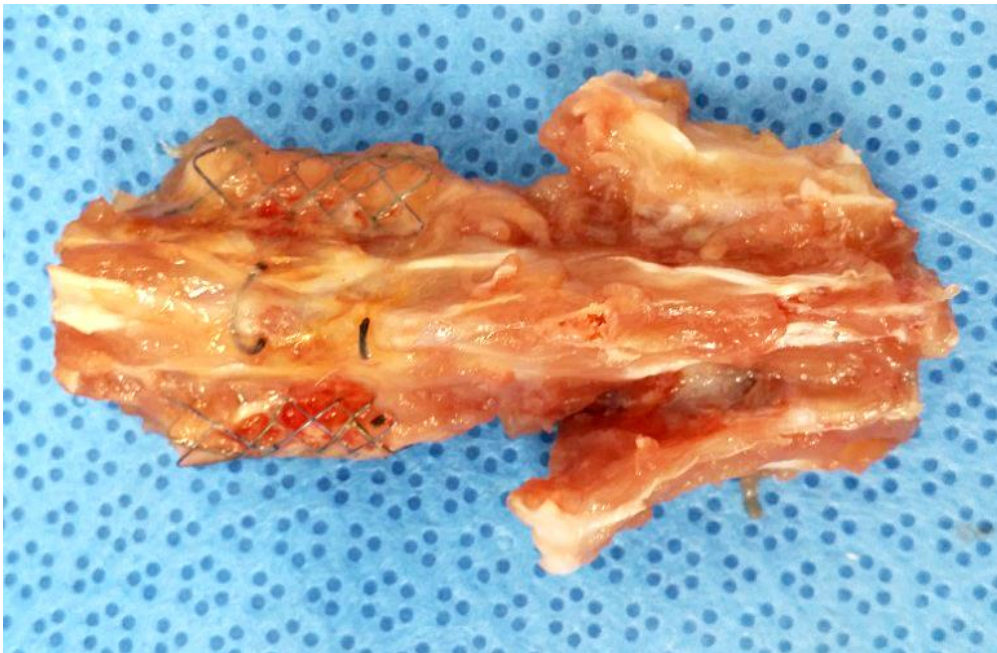


Figure 3C. Lumbar spine was extracted 8 weeks after surgery for fusion assessment.

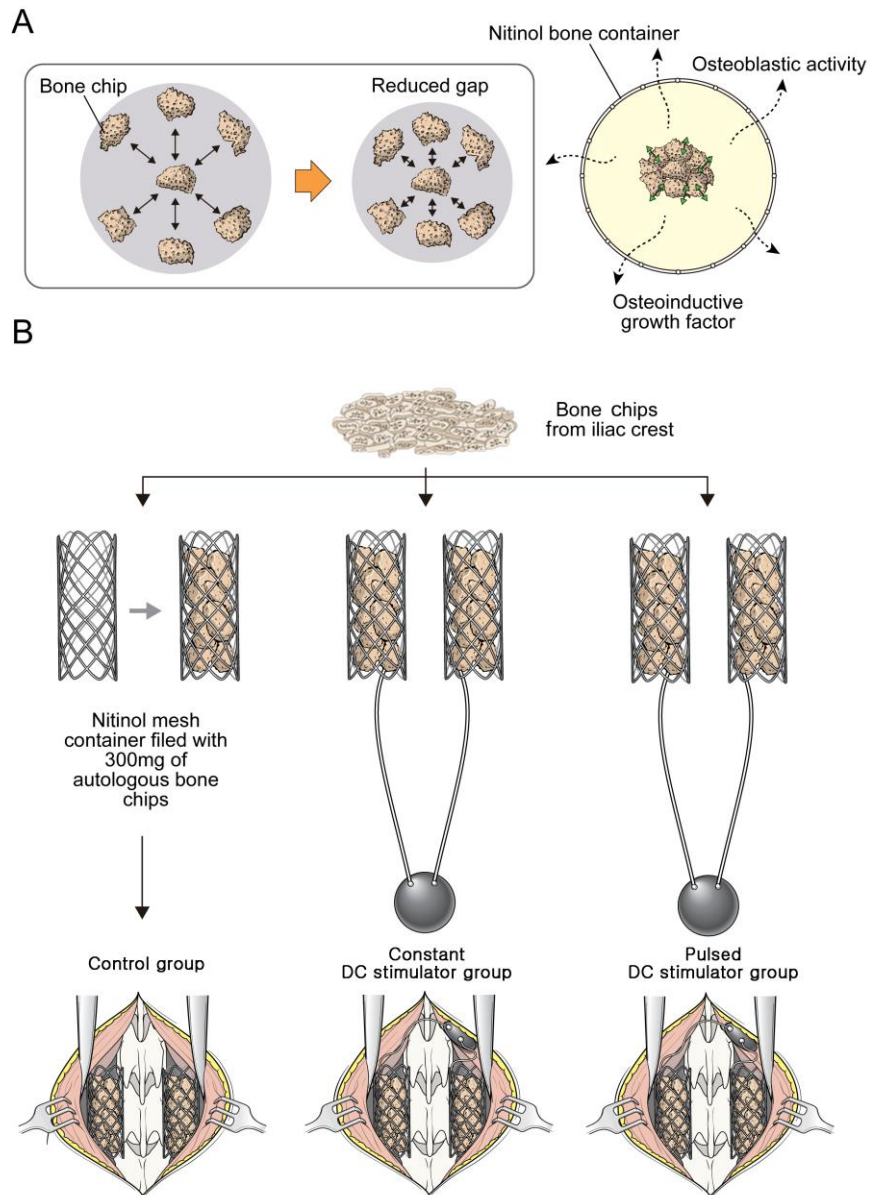


Figure 4. Schematic illustration of rat posterolateral fusion. A. Roles of nitinol mesh were to reduce gaps between bone chips and to prevent soft-tissue interposition. B. Morselized corticocancellous bones were implanted in the space between L4 and L5 transverse processes, using nitinol mesh container with or without varied DC stimulator.

Table 2. Group description

Group	Graft materials	Number of rats
Control	Autologous bone + nitinol mesh	20
Constant	Autologous bone + nitinol mesh+ constant DC stimulator	20
Pulsed	Autologous bone + nitinol mesh+ pulsed DC stimulator	20

5. Microcomputerized tomographic scan

The explanted spines were scanned by high-resolution microcomputed tomography (Micro-CT; NFR-Polaris-G90, NanoFocusRay, Jeonju, Korea) to measure calcified fusion mass at the region of PLF. Micro-CT scan was performed in long axis of the spine at energy of 65 kVp, current of 115 μ A, and exposure time of 34 ms to produce a resolution with voxel size of 27.70 mm^3 . Images were reconstructed using Feldkamp's cone-beam reconstruction algorithm. Size of reconstructed image was 1024 x 1024 pixels, and 512 slices were acquired. Final data were converted to Digital Imaging and Communication in Medicine (DICOM) format. To investigate integrity of bone union, we examined scout, sagittal, and cross-sectional views by DICOM viewer. We created three-dimensional image reconstructions to measure the total volume of fusion mass in both sides for each specimen, using commercial software (Xelis, INFINITT Healthcare, Seoul, Korea).

6. Gross palpation and manual testing

Lumbar spines were removed from the rats *en bloc*. Each fused motion segment was immediately palpated for continuity of fusion mass between transverse processes. Two different observers examined each manually segmented motion by flexion and extension at fusion level, and compared the motions to those of adjacent segments in vertebral column. In order to prevent any mechanical damage to fusion mass, test was conducted carefully. Spine with no intersegmental motion was considered "solid," while spine with any motion detected on either side was assessed to be "not solid."

7. Biomechanical testing

The harvested specimens were evaluated using a three-point bending test by Universal Testing Machine (TO-101, TESTONE, Seoul, Korea). Both ends of vertebral body were placed with their dorsal sides down on two fulcra. Upper anvil (10.0-mm diameter) was placed in a position that applies a load on ventral surface of intervertebral disc perpendicular to longitudinal spine. Three-point bending tests were performed at 40.0-mm intersupport distance and 50-mm/min crosshead speed until upper anvil advanced to 10 mm (Figure 5). The ultimate failure force was recorded as peak load to failure, and stiffness was calculated based on the slope of linear portion of force-displacement curve. Results were statistically compared.

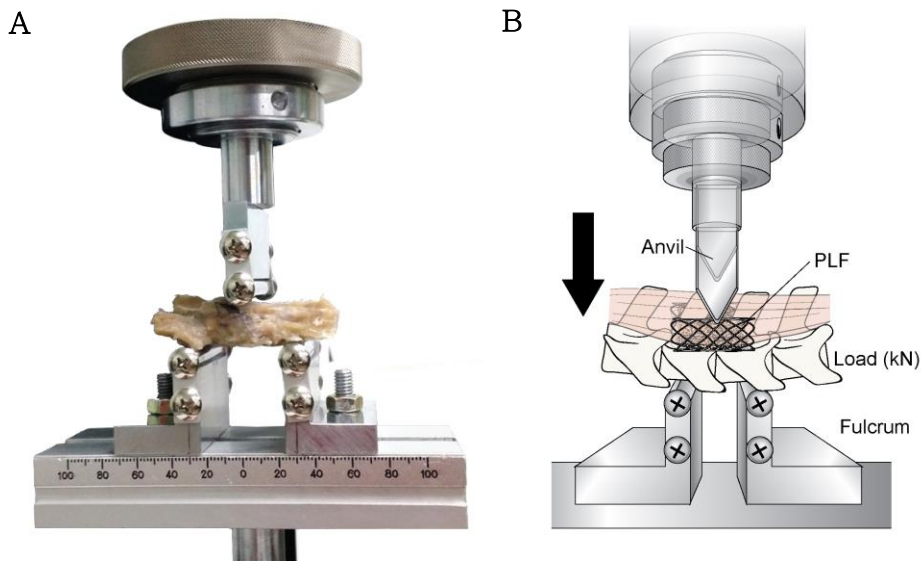


Figure 5. Biomechanical assessment of fusion mass at 8 weeks after posterolateral spinal fusion (PLF) using three-point bending test. A. Experimental setup of three-point bending measurement. B. Arrow indicates direction of force exerted on fusion mass.

8. Histological examination

Sample preparation: Explants were fixed in 10% neutral buffered formalin for 7 days. After being washed, samples were decalcified for 14 days in EDTA at room temperature. Decalcified specimens were used for histological examination. Specimens were fixed in 10% formalin in neutral buffer solution. After fixation, specimens were dehydrated in graduated ethyl alcohol solutions from 70% to 100%. Specimens were then embedded in paraffin, and 4- μ m thick sections were stained with H&E (hematoxylin and eosin) and Goldner's trichrome staining methods. Samples were immersed in 1:1 ratio of absolute ethano and white resin, and then left on a rotor for 1 hour at room temperature. Ethanol/resin mixture was changed three times every hour. These prepared samples were embedded in flat embedding molds made of polytetrafluoroethylene (PTFE), and cut on standard microtome using a motorized ultra-microtome and glass knife (5 mm).

H&E staining: Each tissue was sectioned in 20- μ m thickness, and then stained by H&E staining method. First, frozen section compounds (Leica, Wetzlar, Germany) were removed at each section, followed by nuclei staining using hematoxylin at 37°C for 15 minutes and washing. After that, tissues were differentiated in 0.35% acid alcohol solution, treated by bluing solution that was 1% lithium carbonate, and then washed again. Next, cytosol staining was performed using eosin solution for 5 minutes, followed by washing. Finally, sections were dehydrated by graded ethanol (70% to 100%), and cleared by xylene before mounting. Samples were observed under a light microscope (IX71; Olympus, Tokyo, Japan).

Goldner's trichrome staining: At each step, sample was rinsed in xylene, 100% ethanol, 95% ethanol, and distilled water two times for 2 minutes. Then, sample was placed in Bouin's fluid solution for 1 hour at 56°C. After being rinsed in distilled water, sample was placed in Weigert's hematoxylin for 10 minutes. Sample was then washed in tap water and stained in Ponceau Acid Fuchsin for 5 minutes. Sample was washed in 1% acetic acid, and placed in Phosphomolybdic Acid Orange G solution (Sigma)

until collagen was decolorized. Sample was rinsed in 1% acetic acid, stained in light green stock solution for 5 minutes, and then rinsed again in 1% acetic acid.

Immunohistochemistry: Sections were incubated overnight at 4°C with primary antibody using incubation buffer (1% bovine serum albumin, 1% normal donkey serum, 0.3% Trion[®] X-100, and 0.01% sodium azide in PBS), and then by secondary species-specific fluorescent antibodies for 1 hour at room temperature. After that, sections were mounted by mounting solution (UltraCruzTM Mounting Medium, Santa Cruz Biotechnology, Dallas, Texas). Stained samples were observed under laser confocal microscope (LSM 510; Zeiss, Gottingen, Germany) and Leica microscope (DM 2500; Leica, Wetzlar, Germany).

9. Molecular analysis

Extracts of lumbar 4 to 5 spinal segment, which was previously fused with nitinol mesh and varied DC stimulator, were obtained. Extracted samples were stored at -80°C until protein was ready to be isolated. All surrounding soft tissue was removed and bone was placed on a dry ice block. We pulverized the bone sample into near-powder state using mortar and pestle, while it was placed in liquid nitrogen. Bone powder was then transferred to Eppendorf tube, and stored on ice until it was ready to be lysed. RIPA lysis buffer (Thermo, Waltham, MA) supplemented with protease/phosphatase inhibitors (Thermo) was added, and sample was left on ice for 15 minutes. Following addition of buffer, sample was centrifuged at 13,000g for 15 minutes. We transferred supernatant to a new tube and discarded pellet. Using the newly obtained protein from supernatant, we proceeded with western blotting.

10. Statistical analysis

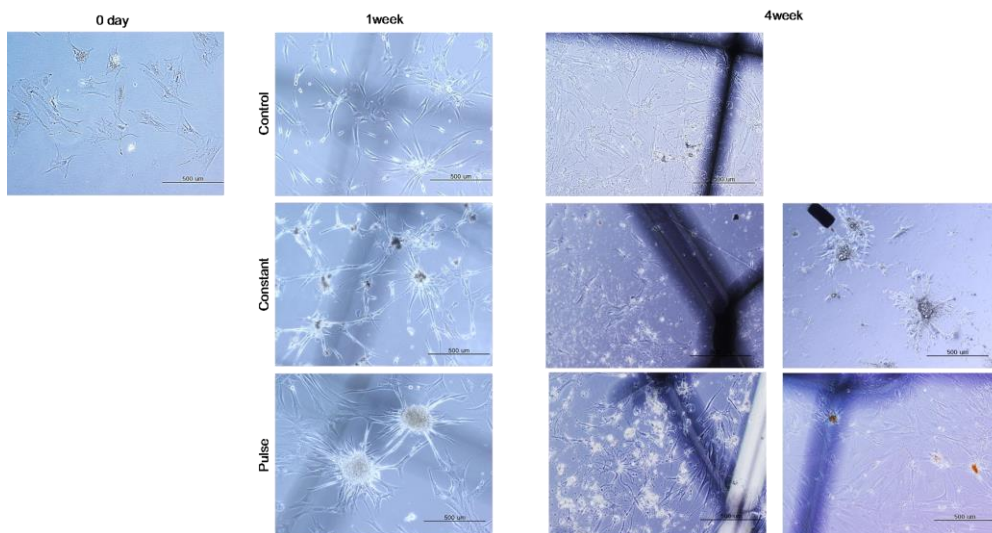
All quantitative data are presented as mean \pm standard deviation. P-value less than 0.05 was considered statistically significant. Statistical significance was analyzed between groups by one-way ANOVA testing. All statistical analyses were performed using SPSS Statistics software, Version 21.0 (IBM, Somers, NY).

III. RESULTS

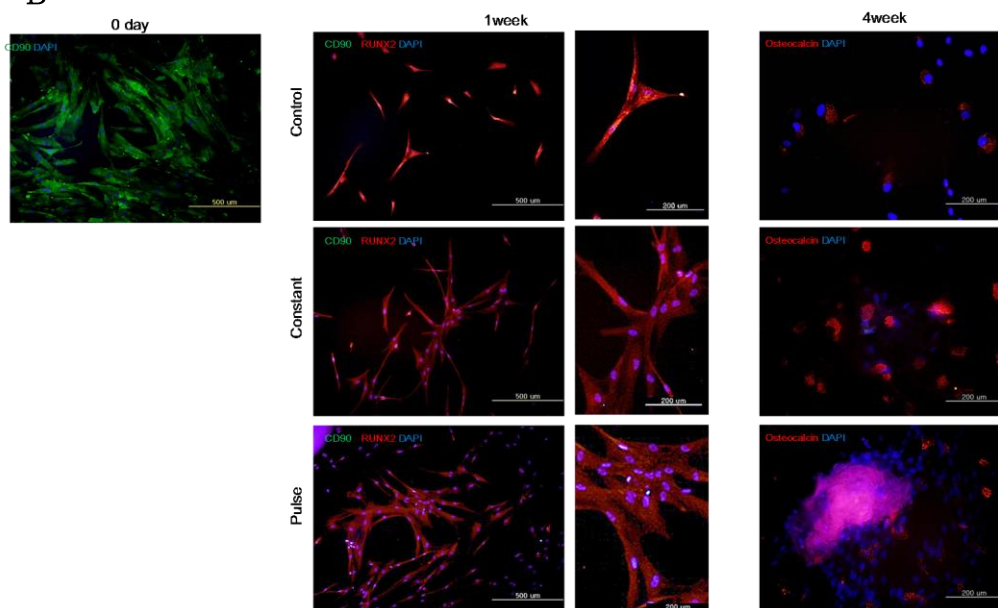
1. Characterization of human mesenchymal stem cell-like cells

In order to identify osteogenic differentiation by electrical stimulation, hMSC-LCs positive for both CD44 and CD90 were cultured in a specifically designed dish, and observed for 1 to 4 weeks. While undifferentiated cells did not show osteogenic differentiation, we observed three dimensional growth of cell mass over a week. Particularly significant growth in this type of mass was detected in pulsed DC stimulator group (Figure 6A). The differentiation of MSC-LCs is compared by the means of immunostaining. When hMSC-LCs originally positive for CD90 begin cell differentiation, they are no longer positive response to CD90 and become positive (red) to RUNX2, a preosteoblast marker. After 4 weeks, Osteocalcin as a marker of mature osteoblasts shows an observable positive response. In alkaline phosphate staining, hMSC-LCs is not successfully stained in the first week. After 4 weeks, the prominent result of staining are shown, which is the osteoblast staining of violet. Cells near by the nitinol mesh observed to be stained in both constant and pulsed DC stimulator groups. In alzarin red staining, Osteocyte was stained with red color. Furthermore, remarkable formation of bone mass adjacent to negative terminal made it clear that there was a strong correlation between bone formation and electrical stimulation. After 4 weeks, we found a substantial difference in pulsed DC stimulator group, in which osteocalcin was successfully stained (Figure 6D).

A



B



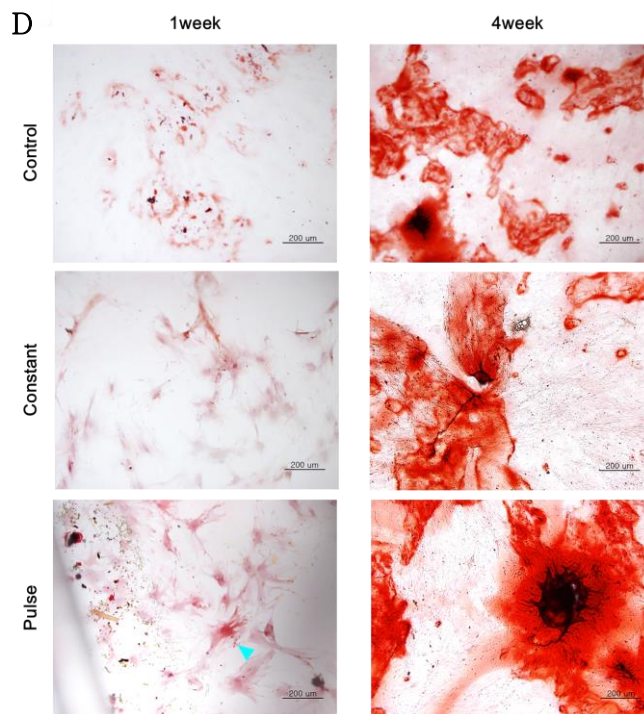
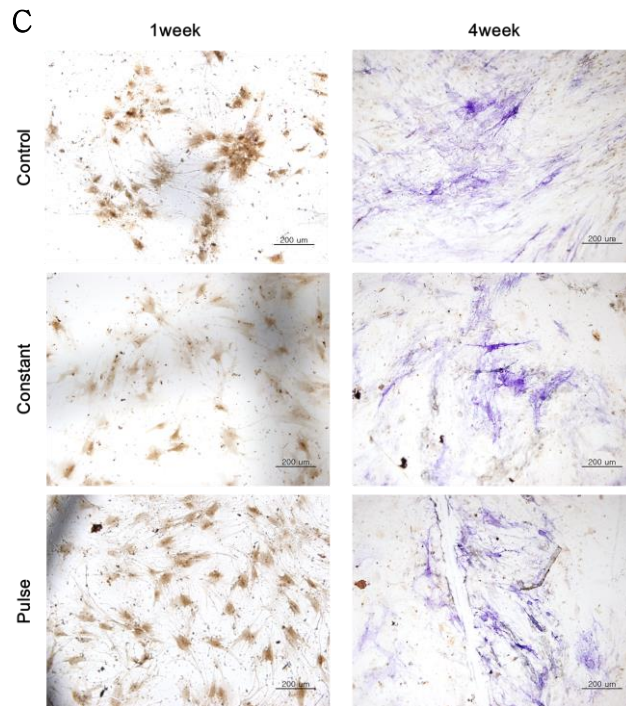


Figure 6. Microscopic images of target cells

A. Microscopic images of hMSC-LCs cultured on nitinol mesh. Pulsed DC stimulator group showed significant growth of cell mass, especially near negative electrode.

B. Immunostaining of cultured groups. Since hMSC-LCs marking cells that were originally positive (green) to CD90 began with differentiation, they no longer showed positive response to CD90 and became positive (red) to RUNX2, a preosteoblast marker. After 4 weeks, noticeably positive response emerged with osteocalcin as marker of mature osteoblast.

C. Alkaline phosphate staining. Osteoblast was stained with violet color. Successfully stained parts were not detected in 1 week. After 4 weeks, prominent result of staining was shown. Cells near nitinol container were shown to be stained in both constant and pulsed DC stimulator groups.

D. Alizarin red staining. Osteocyte was stained with red color. Pulsed DC stimulator group showed most extensive growth along negative nitinol wire.

2. Microcomputerized tomographic scan

Pulsed DC stimulator group showed more extensive new bone formation in fusion mass (Figure 7A). Fusion mass of varied DC stimulator group was fused firmly with adjacent transverse processes, and no crack was observed inside fusion mass. On the other hand, although nitinol container-only group also showed new bone formation, clefts between L4 and L5 transverse processes were observed in subjects with fusions that were “not solid.” Although unremodeled bone chips were also noted in varied DC stimulator group, cortical rims were more well-defined. Analysis of Micro-CT images revealed that the volume of new bone mass varied significantly amongst groups; in order of largest to smallest, they were: pulsed, constant, and control groups (277.6 ± 8.5 mL vs. 263.5 ± 11.8 mL vs. 225.4 ± 20.1 mL, $p < 0.05$, Figure 7B). Differences in size of fusion mass around right side of transverse process near negative terminal showed statistical significance (Rt. is (-) site : 138.4 ± 6.7 mL vs. 134.6 ± 7.5 mL vs. 101.7 ± 14.8 mL, $p < 0.05$, Figure 7B).

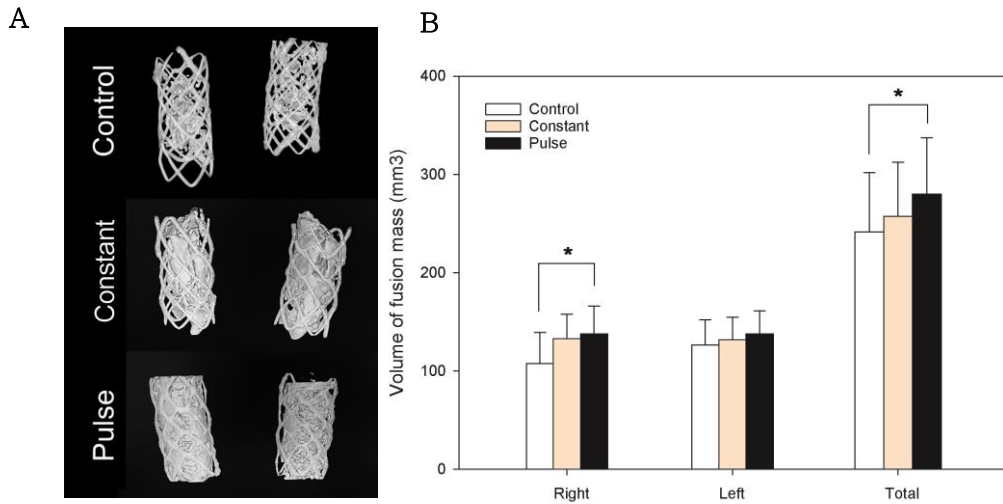


Figure 7. Microcomputed tomography analysis on volume of newly formed bone at 8 weeks after posterolateral fusion. A. Three-dimensional microcomputed tomography images revealed volume of new bone mass. B. Graph illustrating volume of fusion mass. Rt is (-) site and Lt is (+) site. Significantly larger volume of fusion mass was observed in pulse DC stimulator group compared to control group. All values were given as mean \pm STDEV. *Statistical difference was compared between control and pulsed DC stimulator groups. $P < 0.05$ was used for all statistical comparisons.

3. Manual assessment of fusion

Manual palpation after 8 weeks revealed that, overall, 90% (54/60) of explanted spines had solid fusion. Six rats with “not-solid” fusion, all of which belonged to nitinol container-only control group, showed less volume of bony mass on gross inspection and intersegmental motion on manual palpation. In all rats with solid fusion, continuous bony mass was palpated and no intersegmental motion was noted between intertransverse processes. Nitinol container-only control group had solid fusion rate of 70% (14/20), whereas varied DC stimulator group showed significantly higher rate and complete form of fusion in all cases (100%, 40/40, $p < 0.01$). There was no extended bony growth to invade paravertebral muscle dorsally and psoas muscle ventrally.

4. Biomechanical testing

Biomechanical testing was performed to evaluate peak force to failure, as well as stiffness, as determined by force-displacement slope. All control segments at L4–L5 were tested and analyzed as a separate group. The ultimate force required for causing bone fracture was greatest in pulsed DC stimulator group, with 239.46 ± 35.40 N ($p < 0.05$). Levels of force measured in control group and constant DC stimulator group were 143.17 ± 72.60 N and 180.68 ± 36.22 N, respectively (Figure 8A). They demonstrated a mean stiffness of 25.3 ± 9.4 N/mm. In comparison, control group showed stiffness of 16.1 ± 10.6 N/mm, while constant DC stimulator group demonstrated greater stiffness of 23.8 ± 4.4 N/mm, and pulsed DC stimulator group showed even greater stiffness of 31.9 ± 6.2 N/mm (Figure 8B). Pulsed DC stimulator group was found to be significantly stiffer than control group ($p < 0.05$). Stiffness showed a trend very similar to that of ultimate force results.

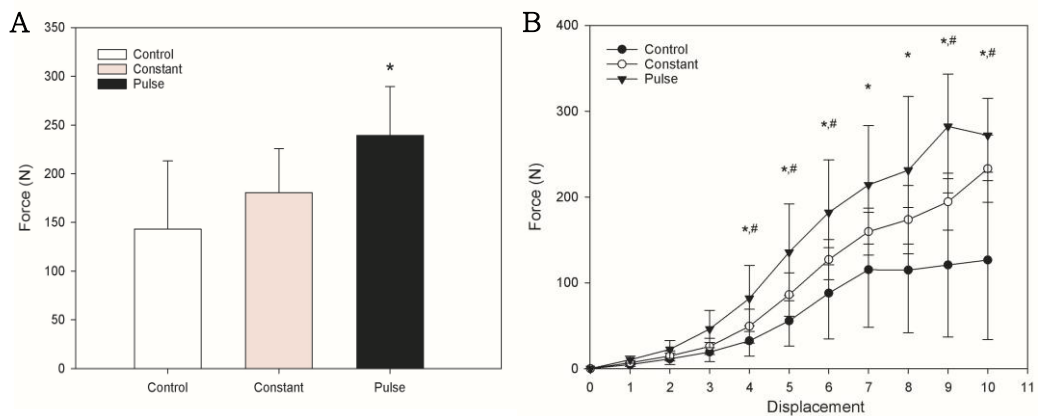


Figure 8. Biomechanical assessment of fusion mass at 8 weeks after posterolateral fusion (PLF) using three-point bending test. A. Average ultimate force to failure of fusion mass for each group. Statistical significance was reached in the amount of force exerted to cause fracture, which was observed to be the greatest in pulsed DC stimulator group compared to those in control and constant DC stimulator groups. B. Force-displacement curves of fusion mass for each group. Pulsed DC stimulator group showed higher stiffness than both control and constant DC stimulator groups. All values are given as means \pm STDEV. *Statistical difference was compared the control

group with the constant and pulsed DC stimulator group. #Statistical difference was compared between constant and pulsed DC stimulator groups. $P < 0.05$ was used for all statistical comparisons.

5. Histological examination

Evaluation of fusion mass was done by immunohistochemistry, H&E staining, and Goldner's trichrome staining methods. Osteocalcin and sclerostin was visualized by immunohistochemistry. Osteocalcin, which is secreted solely by osteoblasts, is thought to play a role in bone mineralization and calcium ion homeostasis. Osteocalcin is used as a preliminary biomarker of bone formation. Similar to results from protein analysis, osteocalcin was most prominent in control group. Results of the current experiment were very different from our expectations. However, pulsed DC group showed higher osteocalcin level than that of constant DC group (Figure 9A). Sclerostin, produced by osteocyte, has anti-anabolic effects on bone formation. Osteocytes are generally acknowledged to sense loading stimuli and regulate processes of remodeling and bone turnover. Sclerostin, which is also an osteocyte maker, was considerably observed in both constant and pulsed DC groups (Figure 9B). Spinal fusion was observed in all three groups by H&E staining. Pulsed DC stimulator group showed higher bone union with peripheral bone than other groups in H&E staining. In addition, H&E staining showed higher disintegration of paravertebral tissue in constant DC group compared to pulsed DC group. In constant DC group, inflammation was observed in bone mass and paravertebral tissue around the stent. Such disintegration was supposed to have resulted from inflammation induced by constant DC stimulation (Figure 9C). In Goldner's trichrome staining, solid fusion was observed in all three groups along nitinol mesh and decorticated transverse processes. Osteoid showed a trend very similar to that of H&E staining results. Orange color showed newly formed, unmineralized "bone-like" dense collagen fibers (osteoid), which will eventually mature and mineralize to form bones (Figure 9D).

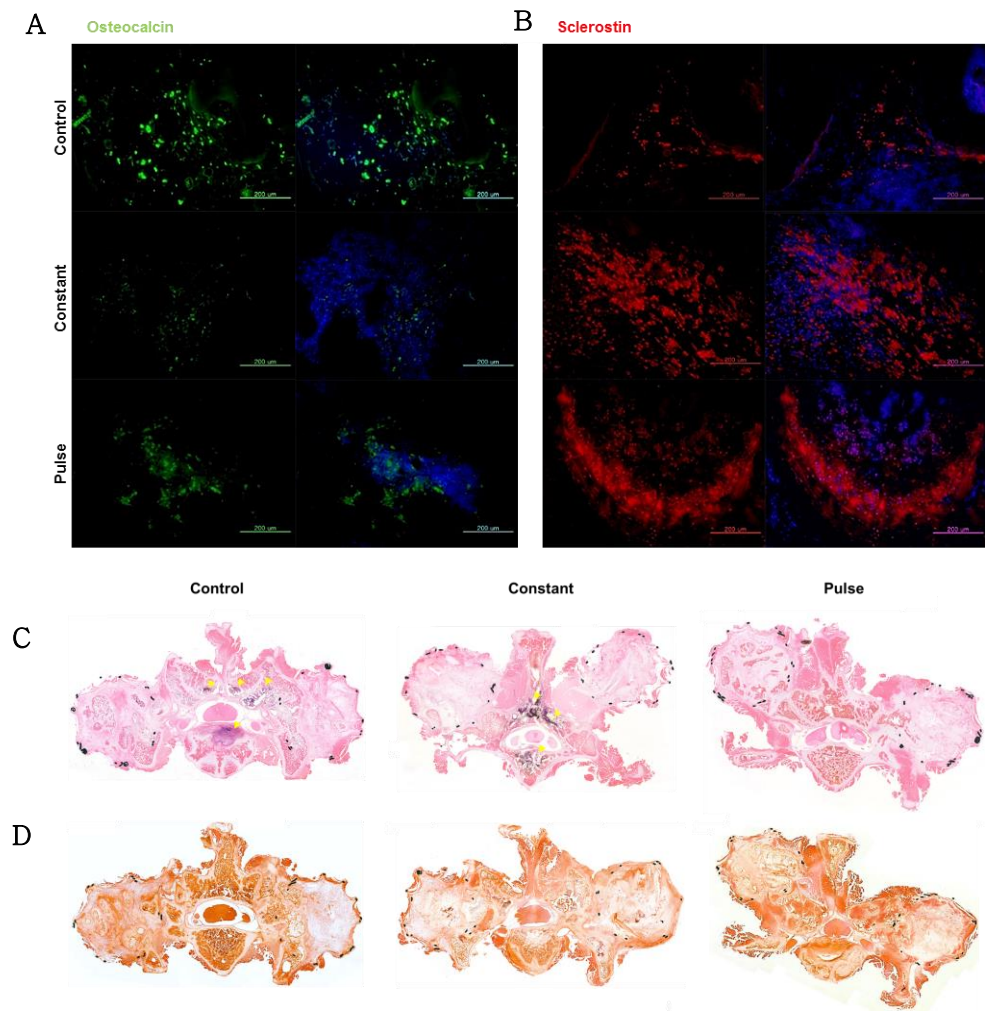


Figure 9. Histological staining of fusion mass at 8 weeks after posterolateral fusion. Control, constant, and pulse groups are shown from left to right. A. Representation of mature osteoblast stained by osteocalcin (green). B. Osteocyte stained by sclerostin (red). C. Hematoxylin and eosin (H&E) staining shows inflammation in the center of spine in constant group (yellow arrow: inflammation region). D. Goldner's trichrome staining shows mature and circuitous osteoid structure (orange color: osteoid region).

6. Molecular analysis

Protein analysis was performed 8 weeks after PLF on bone tissue of identical level using osteocalcin and sclerostin (Figure 10A). Based on the expressed amount of β -actin set as level 1, expressions of osteocalcin, an osteoblast marker, came out to be 0.83, 0.49, and 0.8 in control, constant, and pulse groups, respectively, with no significant differences between results of control and pulse groups. However, expressions of sclerostin, an osteocyte marker, was measured to be 0.77, 0.85, and 0.9 in control, constant, and pulse groups, respectively (Figure 10B). These results demonstrate that at 8 weeks after posterolateral fusion, when electrical stimulation was applied in pulse type, osteocyte becomes the more prominently expressed protein.

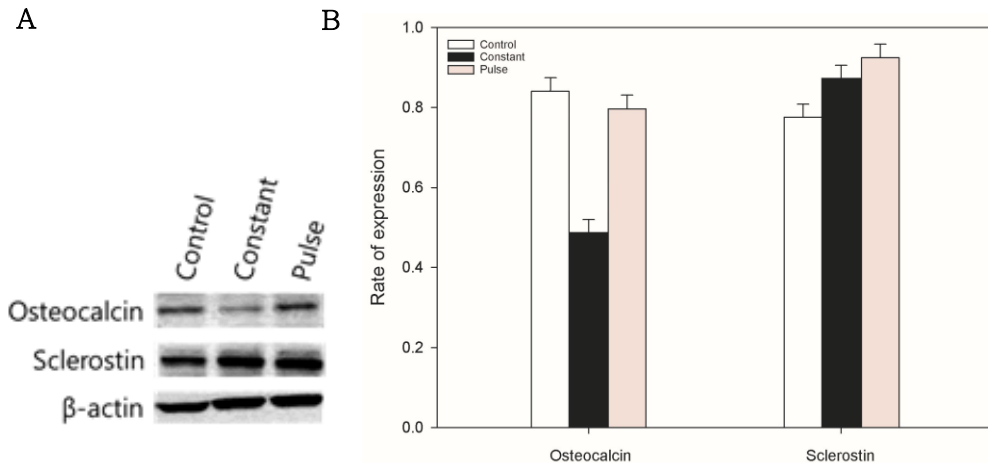


Figure 10. Protein analysis of obtained tissues. A. Western blot of osteocalcin and sclerostin application. B. Expression rates compared between osteocalcin and sclerostin with respect to β -actin. Expression of osteoblast was largely prominent in control group. When it comes to expression of osteocyte, electrical stimulation had a positive role in raising osteocyte expressions in constant and pulse groups compared to control group. Additionally, pulse group showed better expression of osteocyte than constant group.

IV. DISCUSSION

Attainment of reliable fusion is the most important prognostic factor for clinical success in fusion-based posterior lumbar surgery. In conventional spinal fusion surgeries, certain risk factors, such as old age, smoking, multiple-level fusion, and failed prior surgery, have been found to affect fusion rate.²⁴ In particular, geriatric population had more limitations for solid fusion despite use of autograft, as the population had more diabetes, malnutrition, and poor bone quality due to osteoporosis.²⁵ Therefore, alternative methods such as synthetic graft substitutes, tissue-engineered alternatives, tubular mesh container, and electrical stimulation have been designed for use as adjuncts to spinal fusion surgery.²⁶⁻²⁸ For more than 30 years, electrical stimulation has been used to enhance spinal fusions.^{20,27} Since the earliest reported clinical use of electrical stimulation, there has been a growing interest in both clinical and scientific studies on electrical stimulation.¹⁸ Among related techniques, DC electrical stimulation was used the most.²⁹⁻³¹

This study aimed to investigate the effects of varied DC stimulator, such as new bone formation, osteoinductivity, and biologic response, using nitinol container in a rat posterolateral spinal fusion model. Conventional method of PLF execute meticulous decortications of transverse process, as well as piece-by-piece placement of autografts in intertransverse space; consequently, it does not guarantee close and wide contacts between transverse process and graft pieces. To remedy this problem, we built a flexible bone container, made of electrified tubular nitinol mesh, which offered easy contact to irregular surfaces of recipient bones and strong tensile strength as a conductor container that holds bone pieces together. Nitinol container, which can maintain good healing environment for maturation of bone fusion, is still the preferred option for clinical application that eliminates concerns of graft-induced complications. Therefore, an electrified tubular nitinol mesh container, which was applied in this study as a “fusion environment keeper”, may be a promising tool for promoting spinal fusion.²⁶ In this experiment, radiographic images, biomechanical testing, as well as histologic and molecular analyses demonstrated increase in fusion success when

pulsed DC stimulator with nitinol container was used, compared to when only nitinol container with autograft was used. Although new bone formation was observed in all three groups, significantly larger volume and higher strength of new bone showed an increasing trend from nitinol container-only control group to constant, and then to pulsed DC stimulator group. Furthermore, solid fusion was achieved in all cases of varied DC stimulator group, whereas 70% of nitinol container-only group had solid fusion. These figures imply that using varied DC stimulator with nitinol container further strengthened spinal fusion and improved quality of osteogenesis. These results are quite encouraging because the use of varied DC stimulator with nitinol container might reduce the chance of pseudoarthrosis or nonunion, which is reported to occur in 5% to 45% of conventional spinal fusion procedures.^{32,33} Use of adjunctive electrical stimulation to enhance healing of spinal fusion has been shown to be efficacious in both clinical and experimental settings.³⁴

The mechanism by which DC stimulation stimulates osteogenesis has been studied using several animal models. Previous studies using dogs as models have demonstrated statistically significant higher rate of fusion in DC-stimulated specimens by 12 weeks.³⁵ In addition, several recent studies have shown that DC stimulation can enhance fusion success rates in a dose-dependent manner. In a rabbit model using DC in combination with coral-derived bone substitute as an alternative to autograft, Bozic *et al.*³⁶ showed that 100- μ A stimulation by coral was superior to that by autograft. Kahanovitz *et al.*³⁷ developed a facet fusion canine model to show that DC can increase fusion success rates compared to those achieved in unstimulated control subjects and shorten the time to fusion, in a dose-dependent fashion. Similar results were obtained in a pig model.³⁸ However, an authentic electrical current stimulator that can provide optimal results as measured by the ultimate fusion outcome, without tissue necrosis, has yet to be determined. It has been hypothesized that pulsed stimulation, similar to physiologic signal of the human body, delivered to fusion site would result in solid fusion, while having less adverse effects on contiguous bony and soft tissues. This study is the first to provide evidence that pulsed DC stimulation, resembling human heartbeat and synaptic nerve stimulus, can be used

to enhance fusion success. Unlike constant DC stimulation, pulsed DC stimulation will not only maximize the assistive role of effectively fusing damaged bone mass, but also minimize harmful factors that contribute to inflammatory reaction around fusion mass. The above-mentioned hypothesis was proven by high-resolution histological examination. In pulsed DC stimulator group, no evidence of inflammation and necrosis was found within the fused mass of stent or near the site of spinous process. Histologic data were consistent with biomechanical testing results, with pulsed DC stimulator group showing increased bony ingrowth and resorption of autograft in nitinol container compared to other groups. Fabrication of tubular nitinol container was very simple compared to other similar containers, which usually cost more and demand high technology. We used an electrified tubular nitinol mesh that was approved by the Korea Food and Drug Administration. Nitinol mesh has been used in repairing organs, joints, and tissues throughout the body, with low immunological response.³⁹⁻⁴²

Although this study provides novel information regarding the use of varied DC stimulator with nitinol container in a rat PLF, it still has several limitations. First, the spinal biomechanics in a tetrapod animal model differ significantly from those observed in humans. In future studies, a higher-order animal model should be used to assess the effect of these interventions on spinal fusion rates in primates. Second, the accuracy and extent of interobserver agreement for manual palpation testing and radiographic technique have not been extensively evaluated in this preclinical models. Third, inconsistent surgical method could be one of bias for fusion outcome.

V. CONCLUSION

This study showed benefits of using electrical stimulation in a rat spinal fusion model. Pulsed DC stimulation was superior to constant DC stimulation in terms of better fusion rate, higher strength, and lower inflammatory reaction. Future research is required to prove safety and effectiveness of electrical stimulator use in humans.

REFERENCES

1. Boden SD. Overview of the biology of lumbar spine fusion and principles for selecting a bone graft substitute. *Spine (Phila Pa 1976)* 2002; **27**(16 Suppl): S26–31.
2. Gertzbein SD, Hollopeter M, Hall SD. Analysis of circumferential lumbar fusion outcome in the treatment of degenerative disc disease of the lumbar spine. *J Spinal Disord* 1998; **11**(6): 472-8.
3. Rompe JD, Eysel P, Hopf C. Clinical efficacy of pedicle instrumentation and posterolateral fusion in the symptomatic degenerative lumbar spine. *Eur Spine J* 1995; **4**(4): 231-7.
4. Herkowitz HN, Sidhu KS. Lumbar Spine Fusion in the Treatment of Degenerative Conditions: Current Indications and Recommendations. *J Am Acad Orthop Surg* 1995; **3**(3): 123-35.
5. Flouzat-Lachaniette CH, Ghazanfari A, Bouthors C, Poignard A, Hernigou P, Allain J. Bone union rate with recombinant human bone morphogenic protein-2 versus autologous iliac bone in PEEK cages for anterior lumbar interbody fusion. *Int Orthop* 2014; **38**(9): 2001-7.
6. Ito Z, Imagama S, Kanemura T, et al. Bone union rate with autologous iliac bone versus local bone graft in posterior lumbar interbody fusion (PLIF): a multicenter study. *Eur Spine J* 2013; **22**(5): 1158-63.
7. Emery SE, Hughes SS, Junglas WA, Herrington SJ, Pathria MN. The fate of anterior vertebral bone grafts in patients irradiated for neoplasm. *Clin Orthop Relat Res* 1994; (300): 207-12.
8. Boden SD, Martin GJ Jr, Morone M, Ugbo JL, Titus L, Hutton WC. The use of coralline hydroxyapatite with bone marrow, autogenous bone graft, or osteoinductive bone protein extract for posterolateral lumbar spine fusion. *Spine (Phila Pa 1976)* 1999; **24**(4): 320-7.
9. Fu TS, Chen WJ, Chen LH, Lin SS, Liu SJ, Ueng SW. Enhancement of posterolateral lumbar spine fusion using low-dose rhBMP-2 and cultured marrow stromal cells. *J Orthop Res* 2009; **27**(3): 380-4.

10. Nakajima T, Iizuka H, Tsutsumi S, Kayakabe M, Takagishi K. Evaluation of posterolateral spinal fusion using mesenchymal stem cells: differences with or without osteogenic differentiation. *Spine (Phila Pa 1976)* 2007; **32**(22): 2432-6.
11. Taghavi CE, Lee KB, Keorochana G, Tzeng ST, Yoo JH, Wang JC. Bone morphogenetic protein-2 and bone marrow aspirate with allograft as alternatives to autograft in instrumented revision posterolateral lumbar spinal fusion: a minimum two-year follow-up study. *Spine (Phila Pa 1976)* 2010; **35**(11): 1144-50.
12. Ajiboye RM, Hamamoto JT, Eckardt MA, Wang JC. Clinical and radiographic outcomes of concentrated bone marrow aspirate with allograft and demineralized bone matrix for posterolateral and interbody lumbar fusion in elderly patients. *Eur Spine J* 2015; **24**(11): 2567-72.
13. Virk S, Sandhu HS, Khan SN. Cost effectiveness analysis of graft options in spinal fusion surgery using a Markov model. *J Spinal Disord Tech* 2012; **25**(7): E204-10.
14. Hoffmann MF, Jones CB, Sietsema DL. Adjuncts in posterior lumbar spine fusion: comparison of complications and efficacy. *Arch Orthop Trauma Surg* 2012; **132**(8): 1105-10.
15. Thalgott JS, Giuffre JM, Fritts K, Timlin M, Klezl Z. Instrumented posterolateral lumbar fusion using coralline hydroxyapatite with or without demineralized bone matrix, as an adjunct to autologous bone. *Spine J* 2001; **1**(2): 131-7.
16. Bernhardt M, Swantz DE, Clothiaux PL, et al. Posterolateral lumbar and lumbosacral fusion with and without pedicle screw internal fixation. *Clin Orthop Rel Res* 1992; 284: 109-15.
17. Brighton CT, Black J, Friedenberg ZB, et al. A multicenter study of the treatment of nonunion with constant direct current. *J Bone Joint Surg Am* 1981; **63**(1): 2-13.
18. Dwyer AF, Wickham GG. Direct current stimulation in spinal fusion. *Med J Aust* 1974; **1**(3): 73-5.
19. Kane WJ. Direct current electrical bone growth stimulation for spinal fusion. *Spine (Phila Pa 1976)* 1988; **13**(3): 363-5.
20. Rogozinski A, Rogozinski C. Efficacy of implanted bone growth stimulation in instrumented lumbosacral spinal fusion. *Spine (Phila Pa 1976)* 1996; **21**(21): 2479-83.

21. Meril AJ. Direct current stimulation of allograft in anterior and posterior lumbar interbody fusions. *Spine (Phila Pa 1976)* 1994; **19**(21): 2393–8.
22. Boden SD. Biology of lumbar spine fusion and use of bone graft substitutes: present, future, and next generation. *Tissue Eng* 2000; **6**(4): 383-99
23. Poynton AR, Zheng F, Tomin E, et al. Resorbable posterolateral graft containment in a rabbit spinal fusion model. *J Neurosurg* 2002; **97**(4 Suppl): 460–3.
24. Lippman CR, Salehi SA, Liu JC, Ondra SL. Salvage technique of posterior iliac bolt placement in long-segment spinal constructs with a previous posterior iliac crest harvest: technical note. *Neurosurgery* 2006; **58**(1 Suppl): ONS-E178; discussion ONS-E.
25. Gan JC, Glazer PA. Electrical stimulation therapies for spinal fusion: current concepts. *Eur Spine J* 2006; **15**:1301-11.
26. Shin DA, Yang BM, Tae GY, Kim YH, Kim HS, Kim HI. Enhanced spinal fusion using a biodegradable porous mesh container. *The Spine Journal* 2014; **14**(3): 408–15.
27. Drespe IH, Polzhofer GK, Turner AS, Grauer JN. Animal models for spinal fusion. *Spine J* 2005; **5**(6 Suppl): 209S-16S.
28. Bostan B, Gunes T, Asci M, et al. Simvastatin improves spinal fusion in rats. *Acta Orthop Traumatol Turc* 2011; **45**(4): 270-5.
29. Kucharzyk DW. A controlled prospective outcome study of implantable electrical stimulation with spinal instrumentation in a high-risk spinal fusion population. *Spine (Phila Pa 1976)* 1999; **24**(5): 465–9.
30. Tejano NA, Puno R, Ignacio JM. The use of implantable direct current stimulation in multilevel spinal fusion without instrumentation. A prospective clinical and radiographic evaluation with long-term follow-up. *Spine (Phila Pa 1976)* 1996; **21**(16): 1904–8.
31. Mooney V. A randomized double-blind prospective study of the efficacy of pulsed electromagnetic fields for interbody lumbar fusions. *Spine (Phila Pa 1976)* 1990; **15**(7): 708–12.
32. Steinmann JC, Herkowitz HN. Pseudoarthrosis of the spine. *Clin Orthop Relat Res* 1992; **284**: 80–90.

33. Zdeblick TA. A prospective, randomized study of lumbar fusion. Preliminary results. *Spine (Phila Pa 1976)* 1993; **18**(8): 983–91.
34. Dwyer AF, Yau AC, Jeffcoat KW. Use of direct current in spine fusion. *J Bone Joint Surg* 1974; 56A: 442.
35. Dejjardin LM, Kahanovitz N, Arnoczky SP, Simon BJ. The effect of varied electrical current densities on lumbar spinal fusion in dogs. *Spine J* 2001; **1**(5): 341–7
36. Bozic KJ, Glazer PA, Zurakowski D, Simon BJ, Hayes WC, Lipson SJ. In vivo evaluation of coralline hydroxyapatite and direct current electrical stimulation in lumbar spinal fusion. *Spine (Phila Pa 1976)* 1999; **24**(20): 2127–33.
37. Kahanovitz N, Arnoczky S. The efficacy of direct current electrical stimulation to enhance canine spinal fusions. *Clin Orthop* 1990; 251: 295–9.
38. Nerubay J, Margarit B, Bubis JJ, et al. Stimulation of bone formation by electrical current on spinal fusion. *Spine (Phila Pa 1976)* 1986;11:167–9.
39. Wright KC, Wallace S, Charnsangavej C, Carrasco CH, Gianturco C. Percutaneous endovascular stents: an experimental evaluation. *Radiology* 1985; **156**(1): 69-72.
40. Jung GS, Song HY, Seo TS, Park SJ, Koo JY, Huh JD, et al. Malignant gastric outlet obstructions: treatment by means of coaxial placement of uncovered and covered expandable nitinol stents. *J Vasc Interv Radiol.* 2002; **13**(3): 275-83.
41. Odurny A. Colonic anastomotic stenoses and memotherm stent fracture: a report of three cases. *Cardiovasc Intervent Radiol.* 2001; **24**(5): 336-9.
42. Yoon CJ, Song HY, Shin JH, Bae JI, Jung GS, Kichikawa K, et al. Malignant duodenal obstructions: palliative treatment using self-expandable nitinol stents. *J Vasc Interv Radiol.* 2006; **17**(2 Pt 1): 319-26.

ABSTRACT(IN KOREAN)

**백서 후외측 척추유합 모델에서의 전기자극에 의한
요추 체간 유합술의 촉진 효과 분석**

< 지도 교수 김 공 년 >

연세대학교 대학원 의학과

지 규 열

배경내용 : 자가 장골이식술을 이용한 후외측 유합술 (PLF)은 요추 질환에서 가장 흔하게 시행되는 수술 중 하나이다. 그러나, 이식술의 제한된 성공은 새롭고, 생물학적으로 유용한 이식 증강제 또는 대체품을 필요로 하고 있다. 직류 (DC) 전기자극의 사용이 성공적으로 척추 유합율을 증가시키는 것으로 알려졌다. 그러나, 다양한 직류파형의 전기자극기 효과에 대한 정보는 거의 없다.

목 적 : 본 연구는 니티놀 용기에 연결된 다양한 직류파형 전기자극기가 백서 후외측 척추 유합의 강도와 유합률에 미치는 영향을 평가한다.

연구 방법 : 동물 실험 연구.

대상 및 방법 : 관상의 도체 니티놀 망사용기에 백서 장골뼈조각 이식편을 채워 넣었다. 니티놀 메쉬 용기에 다양한 직류파형 전기자극기를 전선으로 연결하여 전기자극을 주었다. 60 마리의 Sprague-Dawley 백서에 양측 장골 이식편을 이용한 L4와 L5 횡돌기 사이에 후외측 유합술을 시행하였다. 전기자극기는 백서의 피하에 이식하였고, 이를 총 3 그룹으로 나누었다 : 니티놀 용기의 대조군은 자가골을 니티놀 용기에 채워 후외측 유합을 시행 (N = 20), 지속파 전기자극군 (100 μ A) 은 자가 이식골을 넣은 니티놀 용기를 지속파 자극기로 연결하여 후외측 유합을 시행 (N = 20), 박동성 전기자극군 (100 μ A, 100Hz, 200 μ s) 은 자가 이식골을 넣은 니티놀 용기를 박동성 자극기로 연결

하여 후외측 융합을 시행 (N = 20). 수술 후 8 주에 희생하여 요추융합 부위를 제거하였다. 척추 융합에 대한 평가는 마이크로 컴퓨터단층촬영, 수지검사, 생역학 검사, 조직학적 검사, 분자생물학적 분석을 진행하였다.

결 과 : 전기자극군의 모든 경우에서 견고한 융합이 이루어졌지만, 니티놀 용기군은 70%의 융합을 보였다. 방사선 사진, 생역학 검사, 조직학 검사 및 분자 생물학적 분석은 니티놀 용기군, 지속과 전기자극군 및 박동성 전기자극군 순서로 척추융합이 증가하는 것을 보여주었다. 신생골양은 박동성 전기자극기군에서 가장 높게 측정되었다 ($p < 0.05$). 융합체의 강도는 박동성 전기자극기군에서 니티놀 용기 대조군보다 더 강하게 융합되어 있었다 ($p < 0.05$). 박동성 전기자극군에서 염증 반응이 가장 적었다.

결 론 : 박동성 직류 전기자극은 백서 후외측 척추융합 모델에서 융합율과 강도를 향상 시키는데 효과적이다. 또한, 관상의 도체 니티놀 메쉬는 작은뼈 이식편의 손실을 줄이고, 양질의 골융합 환경을 유지시키는데 유용하다.

핵심되는 말 : 후외측 융합, 니티놀 망, 전기적 자극, 지속적 전기자극, 박동성 전기자극, 인간 간엽줄기 유사 세포, 골형성 분화